ANALYSIS OF AN ANALOG-DIGITAL CONVERTER WITH A DYNAMIC INTEGRATOR

I. Yu. Sergeev

UDC 621.317.71

In the early 70's the British company Solartron designed the first precision analog-digital converter (ADC) with a dynamic integrator. The same company now manufactures several types of voltmeters based on such ADCs. They include the models 7065, 7071, and 7081; the latter is one of the most accurate voltmeters in the world, correct to 8.5 decimal places. ADCs with dynamic integrators did not get much attention in the literature [1-8]. An analysis carried out by the author [9] proved that the theoretical principles of such ADCs are much more complex than, for example, those of ADCs based on the classical principle of double-slope integration with approximately the same hardware complexity.

Let us analyze the block diagram (Fig. 1) of an ADC with dynamic integration [7, 8]. This ADC includes a three-input integrator, two comparators, two analog switches, and a reversible pulse counter. The voltage U_x to be converted is applied to the first integrator input, and auxiliary alternating square-wave scan voltage U is applied to the second input, and a feedback reference voltage U_E ($+E_1$ or $-E_2$) is applied to the third integrator input through switches controlled by the comparator output signals. The same signals control the inputs of the reversible counter to whose count input are applied pulses of reference frequency f_0. The time diagrams shown in Fig. 2 represent the auxiliary scan voltage U (a), the integrator output voltage U_f (b), the reference voltage U_E at the integrator input (c), and the voltage to be converted U_x (d). The integrator output voltage varies linearly, its slope changing when the comparator voltages reach their threshold level and operate the analog switches. The comparator output voltages also act as the reversible counter control signals t_h and t_ℓ (see notation in Fig. 2) whose duration is the same when $U_x = 0$. If, however, $U_x \neq 0$, then $t_h \neq t_\ell$. The number of reference frequency pulses entering the reversible counter in response to the two control signals is different, the counter code being proportional to the difference between t_h and t_ℓ. The conversion result appears after one square-wave period is completed. If the charges stored by the integrator during one square-pulse period for all three inputs are balanced (i.e., the sum of these charges is zero), we have the equality

$$2U_xT/(R_xC)=\Delta TE/(R_2C),$$

where 2T is the duration of one square-wave period, R_x and R_2 are resistors (see Fig. 1), C is the capacitance of the integrator capacitor, E is the feedback reference voltage ($E_1 = |-E_2| = E$), and ΔT is the difference between the time intervals t_h and t_ℓ.

Hence, the ADC conversion equation has the form

$$\Delta T=2U_xTR_2/(ER_x) \tag{1}$$

or

$$N=U_xN_0R_2/(ER_x), \tag{2}$$

where $N = \Delta T/f_0$ and $N_0 = 2Tf_0$.

The derivation of this equation presumes realization of certain conditions which will be discussed below.

Translated from Izmeritel'naya Tekhnika, No. 6, pp. 38-40, June, 1990.

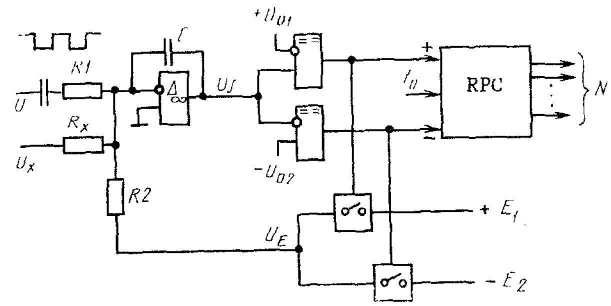

Fig. 1

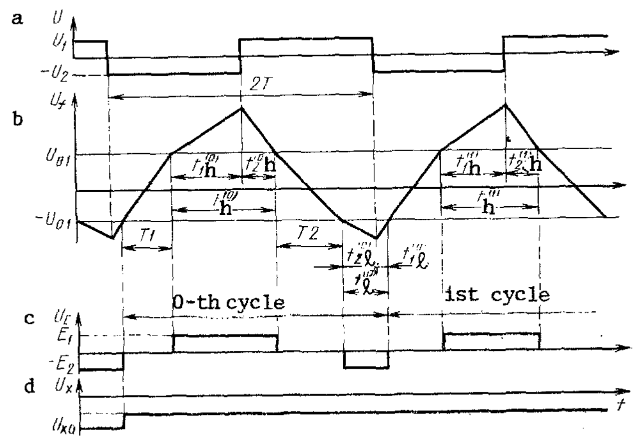

Fig. 2

Let us analyze the ADC operation. Let us assume that at the instant the first ADC operation cycles (square-wave periods) begins the input voltage suddenly changed from $U_x^{(0)}$ to U_x. Let us observe how the time intervals $t_{1\ell}^{(i)}$, $t_{2\ell}^{(i)}$, $t_{2h}^{(i)}$, and $t_{1h}^{(i)}$ (superscript i in parentheses denote the cycle number) vary from cycle to cycle. Obviously, the following equalities are true:

$$t_{1h}^{(1)}=T-T_1-t_{1\ell}^{(0)}, \tag{3}$$

$$t_{2h}^{(1)}=-t_{1h}^{(1)}\frac{U_x-U+E}{U_x+U+E}, \tag{4}$$

$$t_{2\ell}^{(1)}=T-T_2-t_{2h}^{(1)}, \tag{5}$$

$$t_{1\ell}^{(1)}=-t_{2\ell}^{(1)}\frac{U_x+U-E}{U_x-U-E}, \tag{6}$$

$$T_1=-\frac{(U_{01}+U_{02})RC}{U_x-U}=-\frac{2U_0RC}{U_x-U},$$

$$T_2=\frac{(U_{01}+U_{02})RC}{U_x+U}=\frac{2U_0RC}{U_x+U}.$$

Here we assumed that $R_1 = R_2 = R_x = R$; $U_{01} = |-U_{02}| = U_0$; $U_1 = |-U_2| = U$ and $E_1 = |-E_2| = E$.

Successively substituting (5), (4), and (3) into (6) we get an expression for the time interval $t_{1\ell}$ in the first cycle:

$$t_{1\ell}^{(1)}=A_{1\ell}+t_{1\ell}^{(0)}B, \tag{7}$$

where $A_{1\ell}=-(T-T_2)\frac{U_x+U-E}{U_x-U-E}-(T-T_1)B$;

$$B=\frac{(U_x+U-E)(U_x-U+E)}{(U_x-U-E)(U_x+U+E)}.$$

Using (7) as a recurrence formula, we can get expressions for the time interval $t_{1\ell}$ in subsequent cycles:

$$
\begin{aligned}
&t_{1\ell}^{(2)}=A_{1\ell}+t_{1\ell}^{(1)}B=A_{1\ell}(1+B)+t_{1\ell}^{(0)}B^2,\\
&t_{1\ell}^{(3)}=A_{1\ell}+t_{1\ell}^{(2)}B=A_{1\ell}(1+B+B^2)+t_{1\ell}^{(0)}B^3,\\
&\cdots\cdots\cdots\cdots\cdots\cdots\\
&t_{1\ell}^{(n)}=A_{1\ell}+t_{1\ell}^{(n-1)}B=A_{1\ell}\sum_{j=1}^{n}B^{j-1}+t_{1\ell}^{(0)}B^n .
\end{aligned}
\tag{8}
$$

The last expression is seen to have two terms: a geometric progression with the ratio B which converges if $|B| < 1$ and a term $t_{1\ell}^{(0)}B^n$ whose absolute value decreases under the same condition when $n \to \infty$. Thus, if the above inequality is satisfied, $t_{1\ell}$ becomes constant after the transient process ends and can be found applying the well-known formulas of geometric progression:

$$
t_{1\ell}^{(\infty)}=\lim_{n\to\infty}t_{1\ell}^{(n)}=A_{1\ell}/(1-B). \tag{9}
$$

Similarly, for the time interval $t_{2\ell}$ we have

$$
t_{2\ell}^{(1)}=A_{2\ell}+t_{2\ell}^{(0)}BD,
$$

where $A_{2\ell}=-A_{1\ell}\frac{U_x-U-E}{U_x+U-E}=T-T_2+(T-T_1)\frac{U_x-U+E}{U_x+U+E}$;

$$
D=\frac{(U_x-U-E)(U_x^{(0)}+U-E)}{(U_x+U-E)(U_x^{(0)}-U-E)},
$$

$$
t_{2\ell}^{(n)}=A_{2\ell}\sum_{j=1}^{n}B^{j-1}+t_{2\ell}^{(0)}B^nD; \tag{10}
$$

$$
t_{2\ell}^{(\infty)}=\frac{A_{2\ell}}{1-B}\quad\text{or}\quad t_{2\ell}^{(\infty)}=-t_{1\ell}^{(\infty)}\frac{U_x-U-E}{U_x+U-E}. \tag{11}
$$

For the interval t_{2h}:

$$
t_{2h}^{(1)}=T-T_2-A_{2\ell}-(T-T_{20})BD+t_{2h}^{(0)}BD,
$$

where T_{20} is the value of T_2 before the start of the first cycle;

$$
t_{2h}^{(n)}=T-T_2-A_{2h}\sum_{j=1}^{n}B^{j-1}-(T-T_{20})B^nD+t_{2h}^{(0)}B^nD, \tag{12}
$$

$$
t_{2h}^{(\infty)}=T-T_2-\frac{A_{2\ell}}{1-B}\quad\text{or}\quad t_{2\ell}^{\infty}=T-T_2-t_{2\ell}^{(\infty)}. \tag{13}
$$

For the interval t_{1h}:

$$
t_{1h}^{(1)}=-(T-T_2)\frac{U_x+U+E}{U_x-U+E}+A_{1h}+(T-T_{20})BD\,\frac{U_x+U+E}{U_x-U+E}+t_{1h}^{(0)}BD.
$$

where $A_{2h}=A_{2\ell}\frac{U_x+U+E}{U_x-U+E}$; $F=\frac{(U_x+U+E)(U_x^{(0)}-U+E)}{(U_x-U+E)(U_x^{(0)}+U+E)}$.

$$
\begin{aligned}
t_{1h}^{(n)}=&-(T-T_2)\frac{U_x+U+E}{U_x-U+E}+A_{1B}\sum_{j=1}^{n}B^{j-1}+(T-T_{20})\times\\
&\times\frac{U_x+U+E}{U_x-U+H}B^nD-t_{2h}^{(0)}B^nDF,
\end{aligned}
\tag{14}
$$

$$
\begin{aligned}
t_{1h}^{(\infty)}=&-(T-T_2)\frac{U_x+U+E}{U_x-U+E}+\frac{A_{1h}}{1-B}\quad\text{or}\quad t_{1h}^{(\infty)}=\\
&=-t_{2h}\frac{U_x+U+E}{U_x-U+E}.
\end{aligned}
\tag{15}
$$

Using the above expression it is easy to derive the conversion equation of the analyzed ADC. Thus, for steady-state conditions using expressions (9), (11), (13), and (15), we have

$$\Delta T = t_{h}^{(\infty)} - t_{\ell}^{(\infty)} = t_{1h}^{(\infty)} + t_{2h}^{(\infty)} - t_{1\ell}^{(\infty)} - t_{2\ell}^{(\infty)} = 2U_x T/E,$$
$$N = \Delta T f_0 = U_x N_0/E.$$

Substituting for the sake of generality U_x/R_x and E/R_2 for U_x/R and E/R, respectively, we get expressions (1) and (2).

Expressions (8), (10), (12), and (14), which define the dynamic error of the ADC, can be used to describe the output settling process. This error, which takes place when the ADC output code is read before the transients are terminated, can be considerable. The error must be taken into account when ADCs are used as parts of an automatic system.

The discussed ADC is described by the general block diagram proposed by the author in [10].

Let us consider the output settling process. As mentioned above, in response to a change in U_x, the output settles according to a geometric progression. This process converges provided $|B| < 1$. It must, however, be mentioned that the operating range of the given ADC is narrower than the range in which the condition $|B| < 1$ is satisfied. The point is that the slope of the integrator output voltage in the sections corresponding to time intervals t_h and t_ℓ (see Fig. 2) decreases with increasing U_x. If $|U_x| = |U - E|$, this section of the curve becomes horizontal.

To select the operating input voltage range, it is necessary to take into account the nature of the ADC input noise. If there is no noise, the final operating range should be taken as $(0.7\text{-}0.8)U_x$ in order to satisfy the inequality $|U_x| < |U - E|$. The operating range may be even smaller in the presence of noise.

The described ADC was simulated on the basis of expressions derived above (the simulation was carried out using the Turbo Pascal algorithmic language and an IBM PC AT personal computer). The model was also used to analyze the settling process of the ADC output in response to an input voltage change for different circuit parameters. The relative conversion error was tens of percents in one cycle, less than 0.1% in two cycles, less than 0.005% in three cycles, and less than 10^{-6}% after 5-7 cycles. The simulation as well as an analysis of the author's model fully confirmed the above results.

LITERATURE CITED

1. British Patent No. 1434414.
2. British Patent No. 1599249.
3. British Patent No. 1599295.
4. J. Pitman and D. A. Baily, Electron. Tech., 13, No. 5, 99 (1979).
5. Yu. N. Evlanov and A. A. Shakhotin, Izmer. Kontrol'. Avtomat., No. 2 (50), 18 (1984).
6. P. P. Ornatskii, Automatic Measurements and Instruments (Analog and Digital) [in Russian], Vishcha Shkola, Kiev (1986), p. 368.
7. Materials of the Solartron Company Seminar [in Russian], Kiev (1983).
8. Solartron Company Catalog. 7071 and 7081 Precision Digital Voltmeters.
9. I. Yu. Sergeev, Theory and Design of Electronic Voltmeters and Their Verification Tools [in Russian], Abstracts of Scientific Technical Conference, Tallin (1985), p. 92.
10. I. Yu. Sergeev, Analysis and Synthesis of Integrating Instrumental Converters with Iterative Additive Error Correction [in Russian], Author's Abstract of Candidate's Thesis, Kiev (1978).